

Available at [www.sciencedirect.com](http://www.sciencedirect.com)journal homepage: [www.elsevier.com/locate/watres](http://www.elsevier.com/locate/watres)

# Effect of pipe corrosion scales on chlorine dioxide consumption in drinking water distribution systems

Zhe Zhang<sup>a</sup>, Janet E. Stout<sup>a</sup>, Victor L. Yu<sup>b</sup>, Radisav Vidic<sup>a,\*</sup>

<sup>a</sup>Department of Civil and Environmental Engineering, School of Engineering, University of Pittsburgh, 943 Benedum Hall, Pittsburgh, PA 15261, USA

<sup>b</sup>Department of Medicine, School of Medicine, University of Pittsburgh, Pittsburgh, PA, USA

## ARTICLE INFO

### Article history:

Received 11 March 2007

Received in revised form

21 June 2007

Accepted 18 July 2007

Available online 28 August 2007

### Keywords:

Chlorine dioxide

Corrosion scale

Magnetite

Cuprite

## ABSTRACT

Previous studies showed that temperature and total organic carbon in drinking water would cause chlorine dioxide (ClO<sub>2</sub>) loss in a water distribution system and affect the efficiency of ClO<sub>2</sub> for *Legionella* control. However, among the various causes of ClO<sub>2</sub> loss in a drinking water distribution system, the loss of disinfectant due to the reaction with corrosion scales has not been studied in detail. In this study, the corrosion scales from a galvanized iron pipe and a copper pipe that have been in service for more than 10 years were characterized by energy dispersive spectroscopy (EDS) and X-ray diffraction (XRD). The impact of these corrosion scale materials on ClO<sub>2</sub> decay was investigated in de-ionized water at 25 and 45 °C in a batch reactor with floating glass cover. ClO<sub>2</sub> decay was also investigated in a specially designed reactor made from the iron and copper pipes to obtain more realistic reaction rate data.

Goethite ( $\alpha$ -FeOOH) and magnetite (Fe<sub>3</sub>O<sub>4</sub>) were identified as the main components of iron corrosion scale. Cuprite (Cu<sub>2</sub>O) was identified as the major component of copper corrosion scale. The reaction rate of ClO<sub>2</sub> with both iron and copper oxides followed a first-order kinetics. First-order decay rate constants for ClO<sub>2</sub> reactions with iron corrosion scales obtained from the used service pipe and in the iron pipe reactor itself ranged from 0.025 to 0.083 min<sup>-1</sup>. The decay rate constant for ClO<sub>2</sub> with Cu<sub>2</sub>O powder and in the copper pipe reactor was much smaller and it ranged from 0.0052 to 0.0062 min<sup>-1</sup>. Based on these results, it can be concluded that the corrosion scale will cause much more significant ClO<sub>2</sub> loss in corroded iron pipes of the distribution system than the total organic carbon that may be present in finished water.

© 2007 Elsevier Ltd. All rights reserved.

## 1. Introduction

In United States, chlorine dioxide (ClO<sub>2</sub>) was first used as a disinfectant to control taste and odor problems in the 1940s (Aieta and Berg, 1986; Gates, 1998). However, because of high chemical cost and failure and inefficiency of the generation equipment, ClO<sub>2</sub> has not become a widely used primary disinfectant in drinking water treatment facilities during the 1960s and 1970s (Aieta and Berg, 1986; Gates, 1998). Due to the concerns about disinfection byproducts resulting from the use of chlorine in drinking water treatment, ClO<sub>2</sub> is increas-

ingly being considered as an alternative disinfectant for drinking water treatment. The selectivity and oxidation potential makes ClO<sub>2</sub> a desirable alternative to free chlorine. Its biocidal efficiency is equal to or superior to chlorine. Moreover, ClO<sub>2</sub> is effective over a wide pH range and is very effective for removing iron and manganese (Aieta and Berg, 1986; Gates, 1998).

Current applications of ClO<sub>2</sub> in drinking water treatment include the use of ClO<sub>2</sub> for secondary disinfection (Baribeau et al., 2002), nitrification control (McGuire et al., 2006), oxidation of the cyanobacterial hepatotoxin microcystin-LR

\*Corresponding author. Tel.: +1 412 624 1307; fax: +1 412 624 0135.

E-mail address: [Vidic@engr.pitt.edu](mailto:Vidic@engr.pitt.edu) (R. Vidic).

(MC-LR) (Kull et al., 2006) and bromate control in the desalination process (Belluati et al., 2007).

New electrochemical generation systems use electrochemical cassettes and membrane technology to generate stock solution with approximately 500 mg/L  $\text{ClO}_2$  from 25% sodium chlorite solution. The equipment is easy to install and safe to operate in the institutional plumbing system. Several studies have been conducted to evaluate the efficacy and safety of  $\text{ClO}_2$  generated by this electrochemical process for controlling water-borne pathogens in hospital water systems (Srinivasan et al., 2003; Bova et al., 2004; Sidari et al., 2004). These studies showed that  $\text{ClO}_2$  residual in hot water was significantly lower than in cold water. It is possible that faster reaction of  $\text{ClO}_2$  with organic compounds in hot water and high organic load in the hot water contributed to such observations.

However, the loss of  $\text{ClO}_2$  due to corrosion scales has not been studied in detail. Reactions between free chlorine and iron corrosion scales in distribution system have been reported to account for the significant free chlorine loss in the distribution system (Frateur et al., 1999; Hallam et al., 2002; DiGiano and Zhang, 2005). Loss of chlorite in cast-iron pipe loops (Eisnor and Gagnon, 2004) and full-scale drinking water distribution systems containing cast-iron pipes has also been reported (Baribeau et al., 2002).

Iron corrosion scales in water distribution systems have been investigated extensively because iron pipes are commonly used for distributing drinking water. The compounds usually found in iron corrosion scales include goethite ( $\alpha$ - $\text{FeOOH}$ ), lepidocrocite ( $\gamma$ - $\text{FeOOH}$ ), magnetite ( $\text{Fe}_3\text{O}_4$ ), siderite ( $\text{FeCO}_3$ ), ferrous hydroxide ( $\text{Fe}(\text{OH})_2$ ), ferric hydroxide ( $\text{Fe}(\text{OH})_3$ ), ferrihydrite ( $5\text{Fe}_2\text{O}_3 \cdot 9\text{H}_2\text{O}$ ), green rusts (e.g.,  $\text{Fe}_2^{\text{II}}\text{Fe}_2^{\text{III}}(\text{OH})_{12}(\text{CO}_3)$ ) and calcium carbonate (Sarin et al., 2001, 2004a, b; Tang et al., 2006). Previous studies showed that iron corrosion scales generally contain reduced iron, which can react with oxidative disinfectants (Sarin et al., 2001, 2004a, b).  $\text{ClO}_2$  is a strong oxidant and will oxidize ferrous compounds in iron corrosion scales. The reactions of  $\text{ClO}_2$  with corrosion scales will lead to undesirable losses in the disinfectant residual.

In this study, the corrosion scales from a galvanized iron pipe and a copper pipe that have been in service for more than 10 years were characterized by energy dispersive spectroscopy (EDS) and X-ray diffraction (XRD). The impact of corrosion scale materials on  $\text{ClO}_2$  decay was investigated in DI (de-ionized) water at 25 and 45 °C in a batch reactor to simulate the application of  $\text{ClO}_2$  in hot and cold water systems. In addition,  $\text{ClO}_2$  decay was also investigated in a specially designed reactor made from the iron and copper pipes to obtain more realistic reaction rate data.

## 2. Materials and methods

### 2.1. Characterization of corrosion scale on iron and copper pipes

A 30-inch long, 4-inch diameter galvanized iron pipe and a 15-inch long, 2-inch diameter copper pipe that have been in service for at least 10 years were obtained from a local hospital water system and used for this study. The iron pipe

was covered with deposits of corrosion products and heavily tuberculated as shown in Fig. 1a. The copper pipe was comparatively clean (Fig. 1b) and only a thin film of corrosion scale was detected by a scanning electron microscopy (SEM) image (Fig. 1c).

The scales were scraped from the top, middle and bottom layers of the tubercles close to the end of the iron pipe and ground into powder. The scales from the copper pipe were scraped from the copper pipe wall from both ends of the pipe. The elemental composition of the scales was analyzed by EDS using a Philips XL Series 30 scanning electron microscope and an X-ray energy dispersive spectrometer (Philip Analytical Inc., Natick, MA). The XRD patterns of the samples were obtained with a Philips X'PERT diffractometer (Philip Analytical Inc., Natick, MA) using a standard Ni-filtered  $\text{Cu K}\alpha$  radiation source operating at 40 kV and 30 mA X-ray patterns were analyzed using pattern processing software based on the latest Joint Committee on Powder Diffraction Standards (JCPDS) files. Powder samples were also sent to Materials Characterization Laboratory (Pennsylvania State University, University Park, PA) for X-ray photoelectron spectroscopy using a Kratos Axis Ultra X-ray photoelectron spectrometer (Kratos Analytical Inc., Chestnut Ridge, NY) with an X-ray source of monochromatic  $\text{Al K}\alpha$  (1486.6 eV).

### 2.2. Batch and pipe reactor experiment

A cell culture flask (Wheaton Science Products, Millville, NJ) capable of holding 2500 mL of liquid was used as the batch reactor (Fig. 2). A floating glass cover was used to prevent exchange of gases between the headspace and room air and to minimize the volatility of  $\text{ClO}_2$ . Single-port 45-mm red rubber stoppers with a 0.25-inch hole (Wheaton Science Products, Millville, NJ) were used on the side arms as a temperature monitoring port and a sample withdrawal port. The stoppers were sealed gas tight using a 45-mm inlet cap (Wheaton Science Products, Millville, NJ). The reactor and all parts were autoclaved prior to each experiment. The reactor was soaked overnight in 50 mg/L  $\text{ClO}_2$  solution to satisfy disinfectant demand of the reactor material and rinsed with DI water before use.

The experiments were carried out at room temperature, which varied in a very narrow range of  $25 \pm 2$  °C. Hot water temperatures were maintained by heating the flask on the hot plate with a temperature probe feedback. Temperature monitoring was performed using the temperature probe of the hot plate (PMC Industries Inc., San Diego, CA).

The corrosion scale material for these experiments was sampled from the entire scale of the corroded iron pipe and ground to powder without sieving before adding to the batch reactor. Commercial cuprite ( $\text{Cu}_2\text{O}$ ) and  $\text{Fe}_3\text{O}_4$  powder (particle size  $< 5 \mu\text{m}$ ; Sigma-Aldrich, St. Louis, MO) were also used in these batch reactor experiments.

A  $\text{ClO}_2$  generator (Diox, Klenzoid Inc., Conshohocken, PA) provides a concentrated  $\text{ClO}_2$  stock solution. The effluent solution was discarded until the generator achieved a  $\text{ClO}_2$  concentration of approximately 500 mg/L. The  $\text{ClO}_2$  concentration of the concentrated stock solution (fresh stock solution was prepared for each experiment) was monitored using the Hach Method 8138 (0–700 mg/L). The appropriate

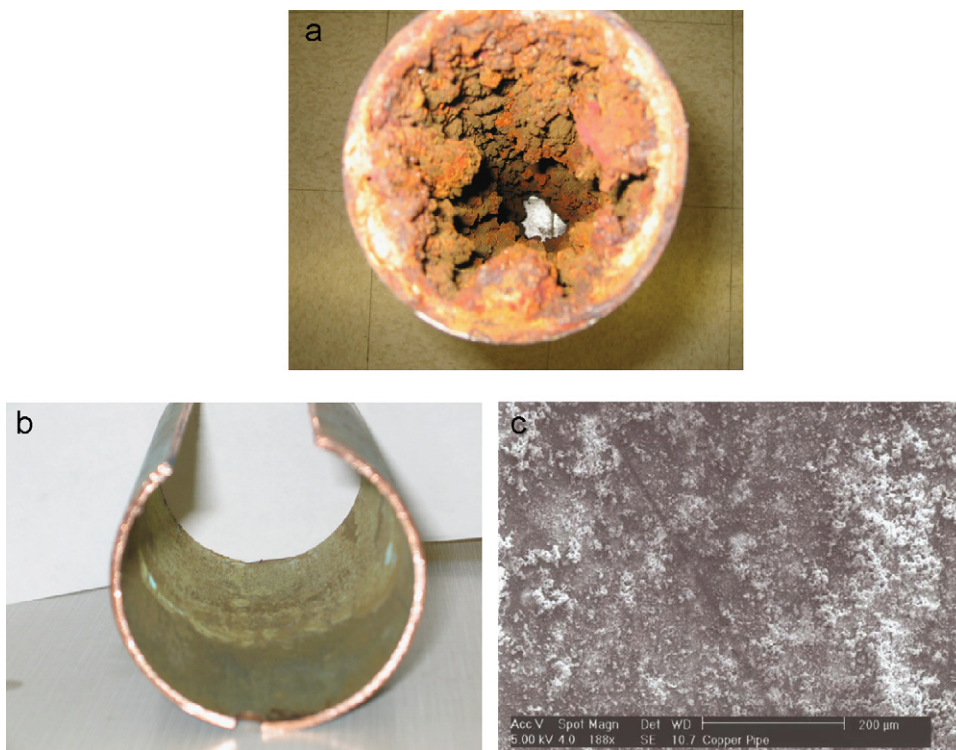


**Fig. 1 – (a) Inner surface of the galvanized iron pipe, (b) inner surface of the copper pipe from a local hospital water system and (c) SEM image of the copper pipe wall.**

amount of the  $\text{ClO}_2$  stock solution was pipetted into the batch reactor to achieve the target  $\text{ClO}_2$  concentration of 1.0 mg/L. The decay of  $\text{ClO}_2$  was monitored after the addition of the corrosion scales using the Hach Method 10101-DPD Method for  $\text{ClO}_2$  (0.00–5.00 mg/L) utilizing a glycine reagent and Hach DPD Free Chlorine Reagent (Hach Company, Loveland, CO). The colorimetric measurements were made using the Hach DR/2010 Spectrophotometer (Hach Company, Loveland, CO).

Samples for chlorite, chlorate and chloride analyses were collected at the beginning and at the end of each experiment. Chlorite, chlorate and chloride were measured by ion chromatography (DX-500, Dionex, Sunnyvale, CA) equipped with a suppressor and conductivity detector according to USEPA Method 300.1. Chlorite, chlorate and chloride concentrations produced through  $\text{ClO}_2$  reaction with corrosion scales were determined as the difference between the final and initial concentrations to eliminate the interference due to the presence of these ions in the stock solution.

pH of the solution was buffered with 0.1 M phosphate buffer and it was adjusted by the addition of 0.1 M NaOH.

Copper and galvanized iron pipes were used to set up the experimental system shown in Fig. 3. Three holes were drilled in the corroded iron and copper pipes and a 0.25-inch plastic tubing was attached as sampling ports. The pipe reactor was flushed with tap water for 24 h before the experiment to re-wet the pipe surface and flush out any easily dislodged tubercles. The flow rate of 1.0 mg/L  $\text{ClO}_2$  stock solution through the pipe was adjusted to achieve the retention time of 10, 20 and 30 min for sampling ports 1, 2 and 3, respectively. The  $\text{ClO}_2$  residual at each sampling port was measured during

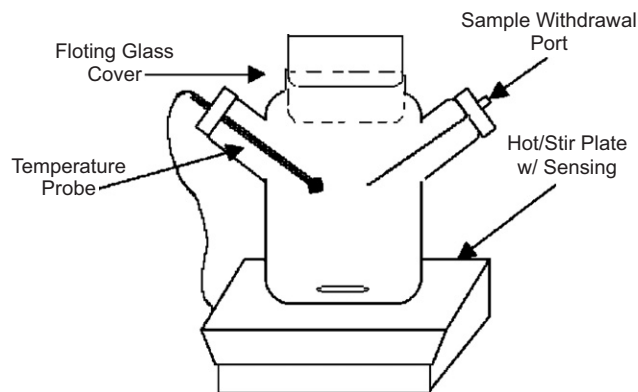


**Fig. 2 – The batch reactor with the floating glass cover.**

the experiment until stable levels were achieved. These experiments were conducted in duplicate to provide statistical validity of the results.

### 3. Results and discussion

#### 3.1. Characterization of corrosion scale

The EDS measurements on powder samples from the galvanized iron pipe identified that iron was the major component element of the scale besides carbon and oxygen. XPS analysis showed that iron was present at 28% (atomic percent), carbon at 18% and oxygen at 48%. The top, middle

and bottom layers of the iron pipe corrosion scale were analyzed by XRD for the changes in compositions and the results are shown in Fig. 4.  $\alpha$ -FeOOH,  $\text{Fe}_3\text{O}_4$ , hematite ( $\alpha\text{-Fe}_2\text{O}_3$ ) and elemental Fe were identified as the main crystalline components. All layers of the scales had a very similar set of peaks, but a few differences were discernible. Comparison of the peak heights for hematite suggests that it is mostly present in the top layer of the scale. Comparing the heights for  $\text{Fe}_3\text{O}_4$  and elemental Fe peaks, it can be inferred that the content of  $\text{Fe}_3\text{O}_4$  and elemental Fe increased from the top layer to the middle layer. The scale structure proposed by Sarin et al. (2004a,b) also included  $\text{Fe}_3\text{O}_4$  as the dominant component in the shell-like layer of iron pipe corrosion scale. Based on these XRD results, it can be concluded that the crystalline ferrous compounds are mainly associated with  $\text{Fe}_3\text{O}_4$ . The lower peak intensity observed for the sample of the bottom layer indicates that the relative quantity of  $\text{Fe}_3\text{O}_4$  is small and that  $\alpha$ -FeOOH is the dominant component in this layer of the scale. Siderite was likely present in minor amounts since it is not stable when exposed to air. These results were similar to the results reported by other research-

ers (Sarin et al., 2001, 2004a,b; Tang et al., 2006). Green rust was not detected in the iron scale since it is not stable and can be further oxidized in contact with air to a more stable phase, like  $\alpha$ -FeOOH or  $\text{Fe}_3\text{O}_4$ .

The EDS measurements on powder samples of the copper pipe scale identified copper as the major component of the scales besides carbon and oxygen. XPS analysis confirmed that copper was present at 10% (atomic percent), carbon at 19% and oxygen at 55%. XRD results showed that the crystalline phase of the copper corrosion scale primarily consists of  $\text{Cu}_2\text{O}$ , copper oxide and metallic copper (Fig. 5).  $\text{Cu}_2\text{O}$  was previously identified as a major corrosion product in copper pipes used in drinking water systems (Merkela et al., 2002). The same study also suggested that light brown  $\text{Cu}_2\text{O}$  film changes to light green malachite fibers ( $\text{Cu}_2\text{CO}_3(\text{OH})_2$ ) by slow oxidation process. Since malachite was not found in the XRD examination of the corrosion samples collected for this study, it is possible that the malachite concentration in the corrosion scale was too low to be detected by XRD.

### 3.2. Reactions of $\text{ClO}_2$ with iron corrosion scale

$\text{ClO}_2$  decay in DI water was first studied to verify the efficiency of the experimental system design with a floating glass cover to minimize  $\text{ClO}_2$  loss due to the volatilization. The mass balance summarized in Table 1 verified that the floating glass cover successfully minimized  $\text{ClO}_2$  loss from the reactor due to volatilization.

The results of  $\text{ClO}_2$  interaction with 1.0 g/L of corrosion scale from the iron pipe at 25 and 45 °C are shown in Fig. 6.

Similar tests were conducted with 2.0 and 5.0 g/L of corrosion scales and the results are summarized in Table 2. A first-order kinetic expression provides a good fit of  $\text{ClO}_2$  decay in DI water containing 1.0, 2.0, 5.0 and 10.0 g/L of pipe

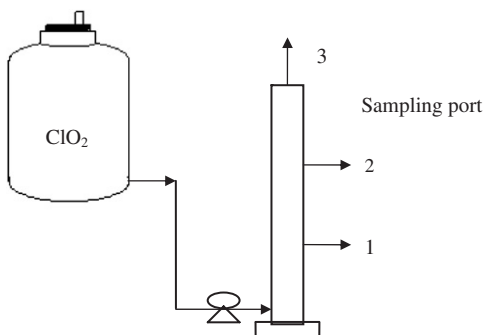


Fig. 3 – The pipe reactor setup.

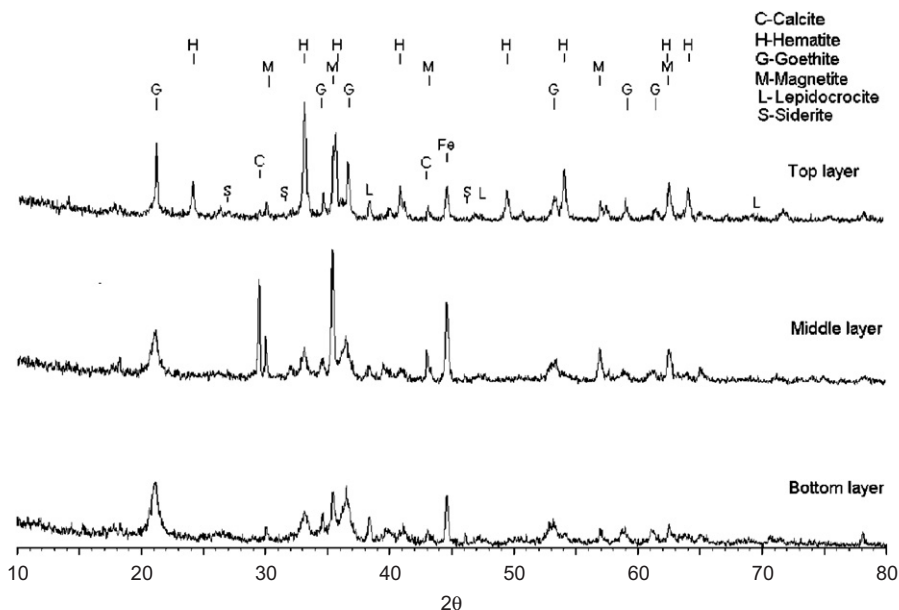


Fig. 4 – XRD patterns of the corrosion scale on different layers of the corroded iron pipe.

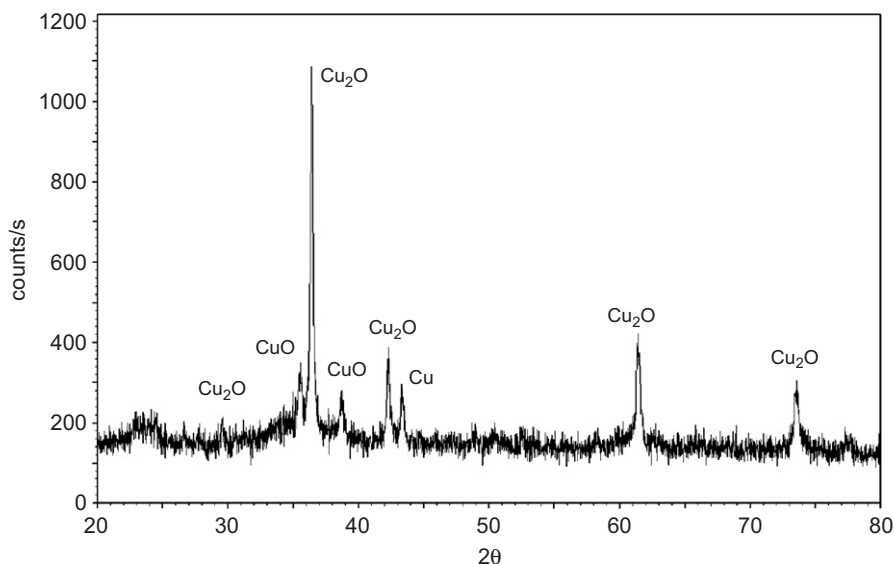


Fig. 5 – XRD patterns of the corrosion scale on the copper pipe.

Table 1 – Mass balance on  $\text{ClO}_2$ , chlorite, chlorate and chloride during the  $\text{ClO}_2$  decay in DI water after 6 h (mg/L)

Test parameters	$\Delta\text{ClO}_2$	$\Delta\text{ClO}_2^-$	$\Delta\text{ClO}_3^-$	$\Delta\text{Cl}^-$	$\text{ClO}_2$ loss due to volatilization <sup>a</sup>
26 °C, pH 7.5	0.04 <sup>b</sup>	0.02	0.01	0.02	-0.01
45 °C, pH 7.5	0.07	0.03	0.02	0.01	0.01
27 °C, pH 8.5	0.03	0.02	0.00	0.01	0
45 °C, pH 8.5	0.06	0.03	0.02	0.01	0

All concentrations are expressed as chlorine.

<sup>a</sup>  $\text{ClO}_2$  loss due to volatility =  $\Delta\text{ClO}_2 - \Delta\text{ClO}_2^- - \Delta\text{ClO}_3^- - \Delta\text{Cl}^-$ .

<sup>b</sup>  $\text{Cl}$  mass = (atomic Cl mass/MW $\text{ClO}_2$ ) $\Delta\text{ClO}_2$ , MW—molecular weight.

corrosion scale over the entire time period (Fig. 6 and Table 2) at 25 and 45 °C. The first-order reaction rate constant for  $\text{ClO}_2$  consumption ranged from 0.025 to 0.083  $\text{min}^{-1}$ . Temperature did not significantly affect the  $\text{ClO}_2$  reaction rate with iron scales since the reaction of  $\text{ClO}_2$  with reduced iron species was very fast.

However, there was a clear relationship between the amount of corrosion scale present in the reactor and the first-order reaction rate constant. Fig. 7 shows that the rate constant increased with increasing scale concentration in the reactor. Such behavior indicates that the availability of corrosion scale in the batch reactor represents the rate-limiting step. The reaction order with respect to scale concentration was investigated using data collected with the initial  $\text{ClO}_2$  concentration of 1.0 mg/L and the scale concentration of 1.0, 2.0, 5.0 and 10.0 g/L. The rate of  $\text{ClO}_2$  decay is described by the pseudo-first-order expression

$$-\frac{d[\text{ClO}_2]}{dt} = k[\text{ClO}_2],$$

where  $k = k'[\text{scale}]^\alpha$ . It is possible to identify the effect of scale concentration on the reaction rate by linearizing the expression for  $k$ :

$$\ln k = \ln k' + \alpha \ln [\text{scale}].$$

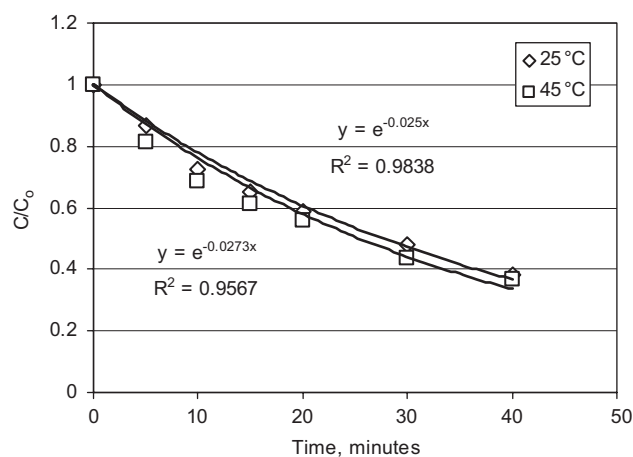
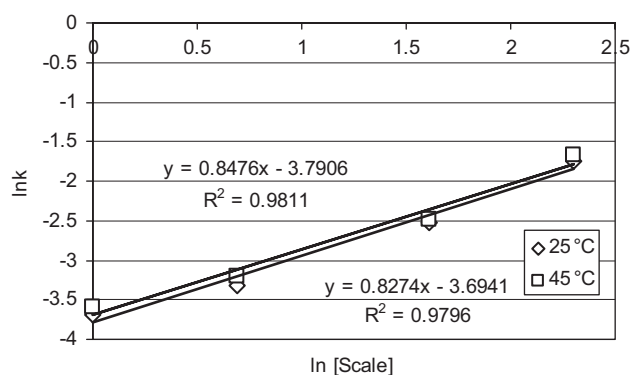


Fig. 6 –  $\text{ClO}_2$  decay in DI water due to reaction with 1.0 g/L of corrosion materials from iron pipe at pH 7.5, 25 and 45 °C.

The reaction order with respect to scale concentration was determined by plotting  $\ln k$  vs.  $\ln [\text{scale}]$ , as shown in Fig. 7. The slope of 0.83–0.85 indicates that the reaction is not exactly of the first order with respect to scale concentration. Based on these results with powder scale from iron pipe, it

**Table 2 – Mean first-order rate constant for the reaction of ClO<sub>2</sub> with the iron corrosion scale, magnetite and cuprite**

Scale concentration (g/L)	Temperature (°C)	Reaction rate constant (min <sup>-1</sup> )	R <sup>2</sup>
1.0	25	0.0251	0.9783
	45	0.0273	0.956
2.0	25	0.0368	0.9913
	45	0.0408	0.977
5.0	25	0.0803	0.9746
	45	0.0829	0.9712
10.0	25	0.1748	0.9748
	45	0.1871	0.9555
1.0 g/L of Fe <sub>3</sub> O <sub>4</sub>	25	0.070	0.9557
	45	0.076	0.9635
2.0 g/L of Cu <sub>2</sub> O	25	0.0052	0.9781
	45	0.0062	0.9745

**Fig. 7 – Impact of iron corrosion scale concentration on the chlorine dioxide decay constant at 25 and 45 °C.**

can be concluded that the rate expression for ClO<sub>2</sub> consumption due to the reaction with the iron corrosion scale has the form

$$-d \frac{[\text{ClO}_2]}{dt} = k' [\text{ClO}_2] \times [\text{scale}]^{0.84},$$

where  $k'$  varies from 0.021 to 0.027 min<sup>-1</sup> (g/L)<sup>-0.84</sup>.

Overall, the reaction of ClO<sub>2</sub> with iron scale follows the first-order reaction kinetics with respect to ClO<sub>2</sub>, but not exactly the first-order reaction with respect to scale concentration (Fig. 7). Such a finding implies a complex reaction mechanism, which is likely due to heterogeneous reactions and the fact that the corrosion scale is a mixture of iron compounds. Compared with the ClO<sub>2</sub> decay rate constant (0.0011–0.0044 min<sup>-1</sup>) in drinking water due to reaction with organic matter (Zhang et al., 2006), the rate constant for the reaction of ClO<sub>2</sub> with the iron pipe corrosion scales (0.0251–0.0829 min<sup>-1</sup>) is almost 20 times greater. Therefore, the major loss of ClO<sub>2</sub> in a water distribution system would be caused by the corrosion scales where heavy corrosion occurred. The decay rate of free chlorine with iron corrosion deposits was

reported to range from 0.0027 to 0.034 h<sup>-1</sup> in the batch reactor (Valentine et al., 2000), which is much smaller than the decay rate of ClO<sub>2</sub> observed in this study.

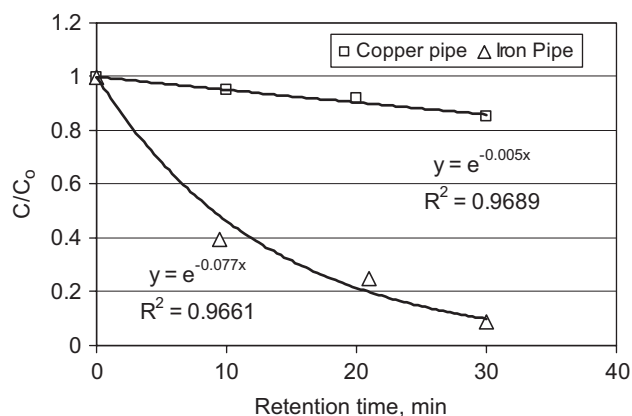
Chlorite analysis showed that 81–95% of ClO<sub>2</sub> was converted to chlorite (Table 3), which suggests that ClO<sub>2</sub> reacts with corrosion scale by a one-electron mechanism whereby ClO<sub>2</sub> oxidizes the ferrous compounds to ferric compounds.

### 3.3. ClO<sub>2</sub> consumption in pipe reactors

The results of the tests with iron and copper pipe reactors (Fig. 3) are shown in Fig. 8. During the first 2 h of the test in the iron pipe, there was no measurable ClO<sub>2</sub> at any of the three sampling ports, which means that ClO<sub>2</sub> was completely consumed in the first 10 inches of the pipe. After approximately 6 h, the mean ClO<sub>2</sub> residual at sampling ports 1, 2 and 3 reached stable levels. Using the first-order kinetic expression to fit the steady-state data, the mean reaction rate constant of 0.077 min<sup>-1</sup> (R<sup>2</sup> = 0.9661) was obtained. It is clear that the reaction between ClO<sub>2</sub> and the corrosion scale was not limited by the concentration of the scale in the pipe

**Table 3 – Mean mass change of ClO<sub>2</sub> and chlorite during the reaction of ClO<sub>2</sub> with the iron corrosion scale, magnetite and cuprite**

Scale concentration (g/L)	Temperature (°C)	ΔClO <sub>2</sub>	ΔClO <sub>2</sub> <sup>-</sup>	ΔClO <sub>2</sub> <sup>-</sup> /ΔClO <sub>2</sub> (%)
1.0	25	0.66	0.63	95
	45	0.66	0.62	94
2.0	25	0.76	0.72	95
	45	0.78	0.74	95
5.0	25	0.93	0.75	81
	45	0.97	0.82	84
1.0 g/L of Fe <sub>3</sub> O <sub>4</sub>	25	0.86	0.74	86
	45	0.91	0.81	90
2.0 g/L of Cu <sub>2</sub> O	25	0.68	0.53	78
	45	0.76	0.65	86

**Fig. 8 – Steady-state ClO<sub>2</sub> residual profile in a used pipe.**

reactor. A similar reaction rate constant was obtained in the batch reactor with an iron scale concentration of 5.0 g/L. The decay rate of free chlorine due to reactions with iron corrosion scale on the pipes (referred to as wall demand to differentiate from bulk decay) ranged from 0.07 to 0.26 h<sup>-1</sup> (Hallam et al., 2002; DiGiano and Zhang, 2005), which is much smaller than that obtained for ClO<sub>2</sub> in this study. Such a behavior is to be expected since ClO<sub>2</sub> is a free radical that is very reactive with ferrous compounds (Moore et al., 2004).

ClO<sub>2</sub> consumption was much slower in the copper pipe than in the iron pipe. After approximately 6 h, the mean ClO<sub>2</sub> residual at sampling ports 1, 2 and 3 reached stable levels that could be modeled using the first-order kinetic expression. The first-order reaction rate constant for the copper pipe of 0.005 min<sup>-1</sup> (R<sup>2</sup> = 0.9689) was obtained. These results suggest that the loss of ClO<sub>2</sub> by the reaction with corroded copper pipe is more than 10 times slower than in the case of corroded iron pipes.

### 3.4. Reactions of ClO<sub>2</sub> with model corrosion scales

Fe<sub>3</sub>O<sub>4</sub> and Cu<sub>2</sub>O were identified as the major components of the corrosion scales collected from iron and copper pipes, respectively. These compounds will cause ClO<sub>2</sub> loss because Fe<sub>3</sub>O<sub>4</sub> has one Fe(II) in each molecule that can be oxidized to Fe(III), while ClO<sub>2</sub> can oxidize cuprous to cupric compounds. The reactions of ClO<sub>2</sub> with Cu<sub>2</sub>O and Fe<sub>3</sub>O<sub>4</sub> were confirmed using commercially available Cu<sub>2</sub>O and Fe<sub>3</sub>O<sub>4</sub> powders with particle size below 5 μm. The reaction rate constant for ClO<sub>2</sub> reaction with 1.0 g/L Fe<sub>3</sub>O<sub>4</sub> was 0.070 min<sup>-1</sup> at 25 °C and it increased slightly to 0.076 min<sup>-1</sup> as the temperature increased from 25 to 45 °C. These values are very close to the ClO<sub>2</sub> decay rate in the iron pipe (Fig. 8) and the reaction rate of ClO<sub>2</sub> with 5 g/L of iron corrosion scale in a batch reactor (Table 2). Therefore, it can be concluded that the reactions between ClO<sub>2</sub> and Fe<sub>3</sub>O<sub>4</sub> in the corrosion scales are likely responsible for most of the ClO<sub>2</sub> loss in the iron pipes. Although Sarin et al. (2001) reported that soluble iron was released to bulk water primarily in the ferrous form, the amount of soluble ferrous ions is typically very small and cannot account for the significant ClO<sub>2</sub> loss observed in this study. Other studies showed that free chlorine loss in the distribution system is also dominated by the reactions with corrosion scale or materials deposited on the surface of the pipe (Valentine et al., 2000).

The corrosion scale on the copper pipe was so limited that it precluded direct experiments in the batch reactor. Because Cu<sub>2</sub>O was identified as the main component of copper corrosion scale, 2.0 g/L of commercial Cu<sub>2</sub>O powder was used to study the reactions between ClO<sub>2</sub> and corrosion scale in copper pipes. The results in Table 3 show that the reactions of ClO<sub>2</sub> with Cu<sub>2</sub>O followed the pseudo-first-order kinetic expression. The reaction rate of ClO<sub>2</sub> with Cu<sub>2</sub>O ranged from 0.005 to 0.006 min<sup>-1</sup>, which is very close to the ClO<sub>2</sub> decay rate observed in the copper pipe (Fig. 8). The reaction rate constant increased to 0.0062 min<sup>-1</sup> as the temperature increased from 25 to 45 °C. The similarity of reaction rate constants suggests that the ClO<sub>2</sub> loss in copper pipe is mostly caused by the reaction of ClO<sub>2</sub> with Cu<sub>2</sub>O that is present in the corrosion scale.

It was found that 78–96% of ClO<sub>2</sub> consumed by the iron corrosion scales, Cu<sub>2</sub>O and Fe<sub>3</sub>O<sub>4</sub> was converted to chlorite (Table 3.), which suggests that ClO<sub>2</sub> reacts with these solids by a one-electron mechanism and oxidizes the ferrous and cuprous ions to ferric and cupric ions, respectively. Concentration of chlorate was negligible and chloride concentration resulting from these reactions could not be determined accurately due to the interference of chloride from corrosion scales. Since chlorite is also a weak oxidant, it can be further reduced to other chlorine species with excess ferrous ions (Hurst and Knocke, 1997; Henderson et al., 2001; Katz and Narkis, 2001), which may explain why the recovery of chlorite decreased as the concentration of corrosion scales increased. Loss of chlorite in full-scale drinking water distribution systems containing cast-iron pipes has already been reported (Baribeau et al., 2002). Chlorite can also react with soluble Fe<sup>2+</sup> and thereby reduce the corrosion rate and red water (Eisnor and Gagnon, 2004).

## 4. Conclusions

Goethite (α-FeOOH) and magnetite (Fe<sub>3</sub>O<sub>4</sub>) were identified as the main components of iron corrosion scale. Cuprite (Cu<sub>2</sub>O) was identified as the major component of copper corrosion scale. The reaction rate of ClO<sub>2</sub> with both iron and copper oxides followed a first-order kinetics. The estimated first-order reaction rate constant for ClO<sub>2</sub> reaction with iron corrosion scales and Fe<sub>3</sub>O<sub>4</sub> ranged from 0.0251 to 0.0829 min<sup>-1</sup>. The estimated first-order reaction rate constant for ClO<sub>2</sub> reaction with Cu<sub>2</sub>O was much smaller and it ranged from 0.005 to 0.006 min<sup>-1</sup>. Fe<sub>3</sub>O<sub>4</sub> and Cu<sub>2</sub>O were likely the main compounds in the scales that caused ClO<sub>2</sub> loss in this study through a one-electron-transfer mechanism. The loss of ClO<sub>2</sub> in the corroded iron pipe is most probably dominated by the reactions between ClO<sub>2</sub> and this ferrous compound present in the corrosion scale. Based on these results, it can be concluded that the corrosion scale will cause much more significant ClO<sub>2</sub> loss in corroded iron pipes of the distribution system than the total organic carbon that may be present in finished water. The application of ClO<sub>2</sub> in the water distribution system using cast-iron pipes is not recommended unless measures to prevent corrosion are fully implemented. Although ClO<sub>2</sub> loss caused by corrosion scale was much slower in the copper pipe than in the iron pipe, it may still be necessary to prevent the corrosion and unnecessary loss of disinfectant due to the corrosion scale in the copper pipe distribution system to maintain effective disinfectant residual.

## REFERENCES

- Aieta, E.M., Berg, D.J., 1986. A review of chlorine dioxide in drinking water treatment. *J. Am. Water Works Assoc.* 78 (6), 62–72.
- Baribeau, H., Prevost, M., Desjardins, R., Lafrance, P., Gates, D.J., 2002. Chlorite and chlorate ion variability in distribution systems. *J. Am. Water Works Assoc.* 94 (7), 96–105.
- Belluati, M., Danesi, E., Petrucci, G., Rosellini, M., 2007. Chlorine dioxide disinfection technology to avoid bromate formation in

- desalinated seawater in potable waterworks. *Desalination* 203 (1–3), 312–318.
- Bova, G., Sharpe, P., Keane, T., 2004. Evaluation of Chlorine Dioxide in Potable Water Systems for *Legionella* Control in an Acute Care Hospital Environment. Engineering Society of Western Pennsylvania, Pittsburgh, PA.
- DiGiano, F.A., Zhang, W., 2005. Pipe section reactor to evaluate chlorine–wall reaction. *J. Am. Water Works Assoc.* 97 (1), 74–85.
- Eisnor, J.D., Gagnon, G.A., 2004. Impact of secondary disinfection on corrosion in a model water distribution system. *J. Water Supply Res. Technol.—Aqua* 53 (7), 441–452.
- Frateur, I., Deslouis, C., Kiene, L., Levi, Y., Tribollet, B., 1999. Free chlorine consumption induced by cast iron corrosion in drinking water distribution systems. *Water Res.* 33 (8), 1781–1790.
- Gates, D., 1998. *The Chlorine Dioxide Handbook*. American Waterworks Association, Denver, CO.
- Hallam, N.B., West, J.R., Forster, C.F., Powell, J.C., Spencer, I., 2002. The decay of chlorine associated with the pipe wall in water distribution systems. *Water Res.* 36 (14), 3479–3488.
- Henderson, R., Carlson, K., Gregory, D., 2001. The impact of ferrous ion reduction of chlorite ion on drinking water process performance. *Water Res.* 35 (18), 4464–4473.
- Hurst, G.H., Knocke, W.R., 1997. Evaluating ferrous iron for chlorite ion removal. *J. Am. Water Works Assoc.* 89 (8), 98–105.
- Katz, A., Narkis, N., 2001. Removal of chlorine dioxide disinfection by-products by ferrous salts. *Water Res.* 35 (1), 101–108.
- Kull, T.P.J., Sjoevall, O.T., Tammenkoski, M.K., Backlund, P.H., Meriluoto, J.A.O., 2006. Oxidation of the cyanobacterial hepatotoxin microcystin-LR by chlorine dioxide: influence of natural organic matter. *Environ. Sci. Technol.* 40 (5), 1504–1510.
- McGuire, M.J., Pearthree, M.S., Blute, N.K., Arnold, K.F., Hoogerwerf, T., 2006. Nitrification control by chlorite ion at pilot scale. *J. Am. Water Works Assoc.* 98 (1), 95–105.
- Merkela, T.H., Grob, H., Werner, W., 2002. Copper corrosion by-product release in long-term stagnation experiments. *Water Res.* 36 (6), 1547–1555.
- Moore, E.R., Bourne, A.E., Hoppe, T.J., Abode, P.J., Boone, S.R., Purser, G.H., 2004. Kinetics and mechanism of the oxidation of iron(II) ion by chlorine dioxide in aqueous solution. *Int. J. Chem. Kinet.* 36 (10), 554–565.
- Sarin, P., Snoeyink, V.L., Bebee, J., Kriven, W.M., Clement, J.A., 2001. Physico-chemical characteristics of corrosion scales in old iron pipes. *Water Res.* 35 (12), 2961–2969.
- Sarin, P., Snoeyink, V.L., Bebee, J., Jim, K.K., Beckett, M.A., Kriven, W.M., Clement, J.A., 2004a. Iron release from corroded iron pipes in drinking water distribution systems: effect of dissolved oxygen. *Water Res.* 38 (5), 1259–1269.
- Sarin, P., Snoeyink, V.L., Lytle, D.A., 2004b. Iron corrosion scales: model for scale growth, iron release and colored water formation. *J. Environ. Eng.* 130 (4), 365–373.
- Sidari, F.P., Stout, J.E., VanBriesen, J.M., Bowman, A.M., Grubb, D., Neuner, A., Wagener, M.M., Yu, V.L., 2004. Keeping *Legionella* out of water systems. *J. Am. Water Works Assoc.* 96 (1), 111–119.
- Srinivasan, A., Bova, G., Ross, T., Mackie, K., Paquette, N., Merz, W., Perl, T.M., 2003. A 17-month evaluation of a chlorine dioxide water treatment system to control *Legionella* species in a hospital water supply. *Infect. Control Hosp. Epidemiol.* 24 (8), 575–579.
- Tang, Z., Hong, S., Xiao, W., Taylor, J., 2006. Characteristics of iron corrosion scales established under blending of ground, surface, and saline waters and their impacts on iron release in the pipe distribution system. *Corros. Sci.* 48 (2), 322–342.
- Valentine, R.L., Vikersland, P.J., Angerman, B.D., Hackett, S.A., Shoup, M., Slattenow, S., 2000. *The Role of the Pipe–Water Interface in DBP Formation and Disinfectant Loss*. AWWA Research Foundation and the American Water Works Association, Denver, CO.
- Zhang, Z., Stout, J.E., Vidic, R.D., 2006. The impact of temperature and TOC on chlorine dioxide decay in drinking water. American Water Works Association Annual Meeting, San Antonio, TX.